

OPTICAL PROPERTIES AND EMISSION CROSS-  
SECTION OF NEODYMIUM NANOPARTICLES  
DOPED TELLURITE GLASS COATED  
WITH GRAPHENE OXIDE/  
REDUCED GRAPHENE  
OXIDE

HAFIZAH RAJAA BINTI SHAARI

UNIVERSITI PENDIDIKAN SULTAN IDRIS

2024

OPTICAL PROPERTIES AND EMISSION CROSS-SECTION OF NEODYMIUM  
NANOPARTICLES DOPED TELLURITE GLASS COATED WITH GRAPHENE  
OXIDE/REDUCED GRAPHENE OXIDE

HAFIZAH RAJAA BINTI SHAARI

THESIS PRESENTED IN FULFILLMENT OF THE REQUIREMENT FOR THE  
DEGREE OF DOCTOR OF PHILOSOPHY

FACULTY OF SCIENCE AND MATHEMATICS  
UNIVERSITI PENDIDIKAN SULTAN IDRIS

2024



Please tick ( )  
Project Paper  
Masters by Research  
Master by Mixed Mode  
PhD

|  |
|--|
|  |
|  |
|  |
|  |

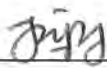
## INSTITUTE OF GRADUATE STUDIES

### DECLARATION OF ORIGINAL WORK

This declaration is made on the .....23...day of...April... 2024

#### i. Student's Declaration:

I, Hafizah Rajaa Binti Shaari, P20191000277, Faculty Of Science And Mathematics hereby declare that the work entitled Optical Properties and Emission Cross-Section of Neodymium Nanoparticles Doped Tellurite Glass Coated with Graphene Oxide/Reduced Graphene Oxide is my original work. I have not copied from any other students' work or from any other sources except where due reference or acknowledgement is made explicitly in the text, nor has any part been written for me by another person.

  
\_\_\_\_\_  
Signature of the student

#### ii. Supervisor's Declaration:

I, Ts. Dr. Muhammad Noorazlan Bin Abd Azis hereby certifies that the work entitled Optical Properties and Emission Cross-Section of Neodymium Nanoparticles Doped Tellurite Glass Coated with Graphene Oxide/Reduced Graphene Oxide was prepared by the above named student and was submitted to the Institute of Graduate Studies as a full fulfillment for the conferment of Doctor of Philosophy (Physics) and the aforementioned work, to the best of my knowledge, is the said student's work.

23 April 2024

Date

  
\_\_\_\_\_  
Signature of the Supervisor

Ts. Dr. MUHAMMAD NOORAZLAN BIN ABD AZIS  
Senior Lecturer  
Physics Department  
Faculty of Science and Mathematics  
Universiti Pendidikan Sultan Idris



**INSTITUT PENGAJIAN SISWAZAH /  
INSTITUTE OF GRADUATE STUDIES**

**BORANG PENGESAHAN PENYERAHAN TESIS/DISERTASI/LAPORAN KERTAS PROJEK  
DECLARATION OF THESIS/DISSERTATION/PROJECT PAPER FORM**

Tajuk / Title: OPTICAL PROPERTIES AND EMISSION CROSS-SECTION OF NEODYMIUM  
NANOPARTICLES DOPED TELLURITE GLASS COATED WITH GRAPHENE  
OXIDE/REDUCED GRAPHENE OXIDE

No. Matrik / Matric's No.: P20191000277

Saya / I: HAFIZAH RAJAA BINTI SHAARI  
(Nama pelajar / Student's Name)

mengaku membenarkan Tesis/Disertasi/Laporan Kertas Projek (Kedoktoran/Sarjana)\* ini disimpan di Universiti Pendidikan Sultan Idris (Perpustakaan Tuanku Bainun) dengan syarat-syarat kegunaan seperti berikut:-

*acknowledged that Universiti Pendidikan Sultan Idris (Tuanku Bainun Library) reserves the right as follows:-*

1. Tesis/Disertasi/Laporan Kertas Projek ini adalah hak milik UPSI.  
*The thesis is the property of Universiti Pendidikan Sultan Idris*
2. Perpustakaan Tuanku Bainun dibenarkan membuat salinan untuk tujuan rujukan dan penyelidikan.  
*Tuanku Bainun Library has the right to make copies for the purpose of reference and research.*
3. Perpustakaan dibenarkan membuat salinan Tesis/Disertasi ini sebagai bahan pertukaran antara Institusi Pengajian Tinggi.  
*The Library has the right to make copies of the thesis for academic exchange.*
4. Sila tandakan ( ✓ ) bagi pilihan kategori di bawah / Please tick ( ✓ ) for category below:-

☐ **SULIT/CONFIDENTIAL**

Mengandungi maklumat yang berdarjah keselamatan atau kepentingan Malaysia seperti yang termaktub dalam Akta Rahsia Rasmi 1972. / Contains confidential information under the Official Secret Act 1972

☐ **TERHAD/RESTRICTED**

Mengandungi maklumat terhad yang telah ditentukan oleh organisasi/badan di mana penyelidikan ini dijalankan. / Contains restricted information as specified by the organization where research was done.

☒ **TIDAK TERHAD / OPEN ACCESS**

  
(Tandatangan Pelajar/ Signature)

Tarikh: 23 April 2024

  
(Tandatangan Penyelia / Signature of Supervisor)  
& (Nama & Cop Rasmi / Name & Official Stamp)  
Dr. MUHAMMAD NOORAZLAN BIN ABDUL AZIS  
Senior Lecturer  
Physics Department  
Faculty of Science and Mathematics  
Universiti Pendidikan Sultan Idris

Catatan: Jika Tesis/Disertasi ini **SULIT @ TERHAD**, sila lampirkan surat daripada pihak berkuasa/organisasi berkenaan dengan menyatakan sekali sebab dan tempoh laporan ini perlu dikelaskan sebagai **SULIT** dan **TERHAD**.

Notes: If the thesis is **CONFIDENTIAL** or **RESTRICTED**, please attach with the letter from the organization with period and reasons for confidentiality or restriction.



## ACKNOWLEDGMENTS

Firstly, and most importantly, I would like to thank Allah the ultimate until the end day comes who has wonderful plans for me and has guided me to here at this moment. He has kept me strong, focused so that I would not go wrong and complete my Ph.D study successfully.

I would like to express my sincere and deep appreciation to my supervisor, Ts Dr Muhammad Noorazlan Abd Azis for his constant encouragement, constructive suggestions and continuous discussion throughout the research. I would also like to extend my sincere appreciation to my co-supervisors Prof Dr Suriani Abu Bakar her support throughout the Ph.D journey.

I would like to extend my gratitude to all of the staff and employees at the Department of Physics and Department of Chemistry, Universiti Pendidikan Sultan Idris. In addition, I would like to extend my appreciation to team members from Instrumentation Unit of Center and Instrumentation Management (i-CRIM) Universiti Kebangsaan Malaysia (UKM), FESEM Laboratory Chemistry Department, Faculty of Science University of Malaya (UM), and NANO-Sci Tech Centre (NST), Universiti Teknologi Mara (UITM), Shah Alam. Special thanks to Dr Nurhafizah Md Disa and Dr. Nur Nabihah Yusof from Universiti Sains Malaysia (USM) for help discussion and kindness during my study

I appreciate all members of the Nanophysics Lab Group at UTM University and other friends for supporting, advising and helping me throughout the years of my graduate study especially Dr Azlina Yahya, Dr Normanisah, and Ms Nur Jannah for support my study

My sincere appreciation goes to Ministry of Education for providing the financial support from Skim Geran Penyelidikan Fundamental (FRGS) Fasa 1/2018 (Grant code: 2019-0006-102-02). Without this support, it is impossible for me to pursue this research with success.

Last and certainly not least, I would like to give my sincere thanks to all the members of my family for their love, continuous support, encouragement and understanding especially my father Mr. Shaari Pandak and Hj Azmi Baharom, my mother Mrs. Azian Abd Majid and Hjh Kamariah Daud. My husband and my sons Eimiza Faisha, Eimiza Hazique, Eimiza Hamza and Eimiza Harraz. Also to my siblings, Atiqah, Muhammad Hanis, Nuruljannah, Munirah and Siti Khadijah for their love, prayer, sacrifices and encouragement during my research period.





## ABSTRACT

This study investigated the optical properties of neodymium nanoparticles (NPs) doped tellurite glass coated with graphene oxide (GO)/ reduced graphene oxide (rGO). Two series of glasses were prepared and coated using melt-quenching and spray-coating methods. The X-ray diffractograms proved the amorphous structure of the glass series. The presence of non-bridging oxygens in the glass network were proven via FTIR analysis. Meanwhile, the existence of neodymium nanoparticles in the tellurite glass network were confirmed using TEM analysis. FESEM and EDX analysis showed the morphologies of GO and rGO on the glass surface and their chemical elements, respectively. From UV-Vis spectroscopy analysis, the optical band gaps of ZBTNd (NPs)-GO and ZBTNd (NPs)-rGO were found in the range 2.355-2.998 eV and 2.770-3.125 eV, respectively. Meanwhile, the refractive index of ZBTNd (NPs)-GO and ZBTNd (NPs)-rGO were 2.041-2.194 and 2.339-2.657, respectively. Furthermore, the oxide ion polarizability ( $\alpha_o^{2-}$ ) of ZBTNd (NPs)-GO and ZBTNd (NPs)-rGO were 3.453-3.854 Å and 3.360-3.664 Å, respectively. The optical basicity ( $\Lambda$ ) values for ZBTNd (NPs)-GO and ZBTNd (NPs)-rGO were 1.220 to 1.262 and 1.174 to 1.214, respectively. The metallization criteria (M) for both glass series demonstrate that the glass system has acceptable optical nonlinearity in the range of  $0.3 < M < 0.4$ . The nephelauxetic ratio ( $\beta$ ) and bonding parameter ( $\delta$ ) indicate the covalency nature in both glass series. The emission cross-section spectra and gains of the neodymium ions ( $\text{Nd}^{3+}$ ) at the transitions of  $^4\text{F}_{3/2} \rightarrow ^4\text{I}_{15/2}$  and  $^4\text{F}_{3/2} \rightarrow ^4\text{I}_{13/2}$  were examined using the McCumber theory. All glass series indicate a positive increase of more than 60% in population inversion. In conclusion, the coating of GO and rGO on the tellurite glass surface gives significant effects on the overall optical properties. Implication of this study is it can offer new advancements in the glass coating field for laser glass.





## SIFAT OPTIK DAN KERATAN RENTAS PELEPASAN BAGI KACA TELURIT DIDOP NEODIMIUM NANOZARAH DISALUT DENGAN GRAFIN OKSIDA/GRAFIN OKSIDA TERTURUN

### ABSTRAK

Kajian ini menyiasat sifat optik kaca telurit didopkan nanozarah (NPs) neodimium bersalut dengan grafin oksida (GO)/ grafin oksida terturun (rGO). Dua siri kaca disediakan dan disalut menggunakan kaedah sepuh lindap dan semburan salutan. Difraktogram sinar-X membuktikan bahawa siri kaca ini mempunyai sifat amorfus. Kehadiran oksigen tidak bersambungan dalam rangkaian kaca telah dibuktikan melalui analisis FTIR. Manakala, kewujudan nanozarah neodimium dalam rangkaian kaca telurit telah disahkan menggunakan analisis TEM. Analisis FESEM dan EDX masing-masing menunjukkan morfologi GO dan rGO pada permukaan kaca dan unsur kimianya. Daripada analisis spektroskopi UV-Vis, jurang jalur tenaga optik ZBTNd (NPs)-GO dan ZBTNd (NPs)-rGO masing-masing didapati dalam julat 2.355-2.998 eV dan 2.770-3.125 eV. Sementara itu, indeks biasan ZBTNd (NPs)-GO dan ZBTNd (NPs)-rGO masing-masing ditentukan dalam julat 2.041-2.194 dan 2.339-2.657. Tambahan pula, kebolehpolaran ion oksida ( $\alpha_o^{2-}$ ) ZBTNd (NPs) - GO dan ZBTNd (NPs) - rGO masing-masing ialah 3.453-3.854 Å dan 3.360-3.664 Å. Nilai kebesan optik ( $\Lambda$ ) untuk ZBTNd (NPs)-GO dan ZBTNd (NPs)-rGO masing-masing ialah 1.220 hingga 1.262 dan 1.174 hingga 1.214. Kriteria perlogaman (M) untuk kedua-dua siri kaca menunjukkan bahawa sistem kaca mempunyai ketidaklinearan optik yang boleh diterima dalam julat  $0.3 < M < 0.4$ . Nisbah nefelauksetik ( $\beta$ ) dan parameter ikatan ( $\delta$ ) menunjukkan sifat kovalen dalam kedua-dua siri kaca. Spektrum keratan rentas pelepasan dan perolehan peralihan ion neodimium  $Nd^{3+}$  pada transisi  ${}^4F_{3/2} \rightarrow {}^4I_{15/2}$  dan  ${}^4F_{3/2} \rightarrow {}^4I_{13/2}$  diuji berasaskan teori McCumber. Semua siri kaca ini menunjukkan peningkatan positif lebih daripada 60% dalam penyongsangan populasi. Kesimpulannya, salutan GO dan rGO pada permukaan kaca telurit memberikan kesan yang signifikan kepada sifat optik secara keseluruhan. Implikasi kajian ini adalah ia dapat menawarkan kemajuan yang baru dalam bidang salutan kaca dalam kaca laser.





## CONTENTS

|                                     | <b>Page</b> |
|-------------------------------------|-------------|
| <b>DECLARATION OF ORIGINAL WORK</b> | ii          |
| <b>DECLARATION OF THESIS</b>        | iii         |
| <b>ACKNOWLEDGMENTS</b>              | iv          |
| <b>ABSTRACT</b>                     | v           |
| <b>ABSTRAK</b>                      | vi          |
| <b>CONTENTS</b>                     | vii         |
| <b>LIST OF TABLES</b>               | xv          |
| <b>LIST OF FIGURES</b>              | xix         |
| <b>LIST OF ABBREVIATIONS</b>        | xxix        |
| <b>LIST OF APPENDICES</b>           | xxxii       |
| <b>CHAPTER 1 INTRODUCTION</b>       |             |
| 1.1 Introduction                    | 1           |
| 1.2 Research Background             | 3           |
| 1.3 Research Problems               | 11          |





|     |                                   |    |
|-----|-----------------------------------|----|
| 1.4 | Research Objectives               | 14 |
| 1.5 | Significance of the Study         | 15 |
| 1.6 | Scope and Limitation of The Study | 16 |
| 1.7 | Thesis Outline                    | 17 |

## CHAPTER 2 LITERATURE REVIEW

|       |   |    |
|-------|---|----|
| 2.1   | Introduction  | 19 |
| 2.2   | Glass Overview  | 20 |
| 2.3   | Glass Preparation Technique.                                  | 25 |
| 2.3.1 | Melt-Quenching  | 27 |
| 2.4   | Tellurite Based Glasses                                       | 30 |
| 2.5   | Borate Oxide  | 33 |
| 2.6   | Zinc Oxide  | 36 |
| 2.7   | Neodymium Rare-Earth Ions (REIs) Doped Glasses System         | 37 |
| 2.8   | Carbon Based Materials  | 39 |
| 2.8.1 | Graphene Oxide and Reduced Graphene Oxide                     | 39 |
| 2.8.2 | Synthesis Method of Graphene Oxide and Reduced Graphene Oxide | 43 |
| 2.8.3 | Deposition Techniques of GO or rGO                            | 44 |
| 2.8.4 | Characteristic Of GO and rGO                                  | 45 |



|        |  |    |
|--------|--|----|
| 2.8.5  | Application of Carbon Based Materials  | 51 |
| 2.9    | Physical Properties Characterization   | 53 |
| 2.9.1  | Density and Molar Volume   | 53 |
| 2.9.2  | Oxygen Packing Density (OPD)   | 57 |
| 2.9.3  | The Ion Concentration of Neodymium (N),<br>Inter-ionic Distance ( $R_i$ ), Polaron Radius<br>( $R_p$ ) | 60 |
| 2.10   | Structural Properties of Glass Materials and Bonding<br>Characterization                               | 62 |
| 2.10.1 | X-Ray Diffraction (XRD)  | 62 |
| 2.10.2 | Fourier Transform Infrared (FTIR)  | 65 |
| 2.10.3 | Transmission Electron Microscopy   | 70 |
| 2.10.4 | Nephelauxetic Ratio and Bonding Parameter  | 72 |
| 2.11   | Optical Properties Characterization  | 73 |
| 2.11.1 | Optical Absorption Spectra   | 73 |
| 2.11.2 | Extinction Coefficient (k)   | 76 |
| 2.11.3 | Optical Energy Bandgap   | 78 |
| 2.11.4 | Refractive Index   | 81 |
| 2.11.5 | Urbach Energy  | 83 |
| 2.11.6 | Electronic Polarizability  | 85 |
| 2.11.7 | Oxide Ion Polarizability   | 87 |

|         |   |    |
|---------|---|----|
| 2.11.8  | Optical Basicity  | 89 |
| 2.11.9  | Metallization Criterion   | 90 |
| 2.11.10 | Reflection Loss ( $R_L$ ), Dielectric Constant ( $\epsilon$ ), Transmission Coefficient (T) | 92 |
| 2.11.11 | Optical Electronegativity   | 94 |
| 2.12    | Absorption and Emission Cross -Section  | 94 |
| 2.12.1  | Gain Properties   | 97 |
| 2.13    | Summary   | 98 |

## CHAPTER 3 METHODOLOGY

|       |  |     |
|-------|--|-----|
| 3.1   | Introduction                                     | 103 |
| 3.2   | Glass Preparation                                | 105 |
| 3.3   | Graphene Oxide Synthesis                         | 108 |
| 3.4   | Reduction Method of GO To Reduced Graphene Oxide | 109 |
| 3.5   | Glass Deposition Process Via Spraying Coating    | 110 |
| 3.6   | Samples Characterizations                        | 112 |
| 3.6.1 | X-Ray Diffraction                                | 112 |
| 3.6.2 | Fourier Transform Infrared (FTIR) Spectroscopy   | 113 |
| 3.6.3 | Transmission Electron Microscopy                 | 115 |
| 3.6.4 | Density Measurement                              | 116 |



|       |   |     |
|-------|---|-----|
| 3.6.5 | Field Emission Scanning Electron Microscope (FESEM) | 116 |
| 3.6.6 | Raman Spectroscopy                                  | 117 |
| 3.6.7 | Energy Dispersive X-ray (EDX)                       | 118 |
| 3.6.8 | Ultraviolet -Visible Spectroscopy                   | 119 |
| 3.7   | Summary   | 122 |

## CHAPTER 4 RESULTS AND DISCUSSIONS

|       |  |     |
|-------|--|-----|
| 4.1   | Introduction   | 123 |
| 4.2   | Physical and Structural of ZBTNd (NPS)-Uncoated Glass  | 124 |
| 4.2.1 | Density and Molar Volume   | 124 |
| 4.2.2 | Oxygen Packing Density (OPD), Neodymium Ion Concentration, Interionic Distance, and Polaron Radius | 127 |
| 4.2.3 | Fourier Transform Infrared (FTIR) Analysis   | 131 |
| 4.2.4 | Transmission Electron Microscopy Analysis  | 135 |
| 4.2.5 | X-ray Diffraction (XRD)  | 136 |
| 4.3   | Structural Properties of ZBTNd (NPs)-GO Glasses  | 138 |
| 4.3.1 | Field Emission Scanning Electron Microscopy Analysis   | 138 |
| 4.3.2 | Energy Dispersive X-Ray Analysis   | 141 |
| 4.3.3 | Micro-Raman Analysis   | 144 |



|        |   |     |
|--------|---|-----|
| 4.4    | Optical Properties of ZBTNd (NPs)-GO Glasses                          | 146 |
| 4.4.1  | Optical Absorption Spectra  | 146 |
| 4.4.2  | Extinction Coefficient, K   | 150 |
| 4.4.3  | Optical Band Gap Energy   | 151 |
| 4.4.4  | Fermi energy, $F_E$   | 155 |
| 4.4.5  | Urbach energy, $\Delta E$   | 156 |
| 4.4.6  | Refractive Index  | 158 |
| 4.4.7  | Reflection Loss, Transmission Coefficient,<br>and Dielectric Constant | 160 |
| 4.4.8  | Nephelauxetic Ratio ( $\beta$ ) And Bonding<br>Parameter ( $\delta$ ) | 163 |
| 4.4.9  | Optical Electronegativity, $\Delta\chi^*$                             | 164 |
| 4.4.10 | Electronic Polarizability   | 166 |
| 4.4.11 | Oxide Ion Polarizability  | 168 |
| 4.4.12 | Optical Basicity  | 171 |
| 4.4.13 | Metallization Criterion   | 173 |
| 4.5    | McCumber Theory and Gain Coefficient of ZBTNd<br>(NPs)-GO Glasses     | 175 |
| 4.5.1  | Absorption Cross-Section And Emission<br>Cross-Section                | 175 |
| 4.5.2  | Gain Coefficient of ZBTNd (NPs)-GO<br>Glasses                         | 184 |
| 4.6    | Structural Properties of ZBTNd (NPs)-rGO Glasses                      | 191 |



|        |  |     |
|--------|--|-----|
| 4.6.1  | Field Emission Scanning Electron Microscopy (FESEM)                | 191 |
| 4.6.2  | Energy Dispersive X-Ray Analysis                                   | 194 |
| 4.6.3  | Micro-Raman Analysis   | 197 |
| 4.7    | Optical Properties of ZBTNd (NPs)-rGO glasses                      | 198 |
| 4.7.1  | Optical Absorption Spectra   | 198 |
| 4.7.2  | Extinction Coefficient, K  | 202 |
| 4.7.3  | Optical Band Gap Energy  | 203 |
| 4.7.4  | Fermi Energy, $F_E$  | 205 |
| 4.7.5  | Urbach Energy, $\Delta E$  | 206 |
| 4.7.6  | Refractive Index   | 208 |
| 4.7.7  | Reflection Loss, Transmission Coefficient, and Dielectric Constant | 210 |
| 4.7.8  | Nephelauxetic Ratio ( $\beta$ ) and Bonding Parameter ( $\delta$ ) | 212 |
| 4.7.9  | Optical Electronegativity  | 213 |
| 4.7.10 | Electronic Polarizability  | 215 |
| 4.7.11 | Oxide Ion Polarizability   | 216 |
| 4.7.12 | Optical Basicity   | 218 |
| 4.7.13 | Metallization Criterion  | 220 |
| 4.8    | Mccumber Theory and Gain Coefficient of ZBTNd (NPs)-rGO Glasses    | 221 |



|       |   |     |
|-------|---|-----|
| 4.8.1 | Absorption Cross-Section and Emission Cross-Section               | 221 |
| 4.8.2 | Gain Coefficient  | 229 |
| 4.9   | Comparative studies of ZBTNd (NPs)-GO and ZBTNd (NPs)-rGO Glasses | 236 |
| 4.9.1 | FESEM Morphology and EDX Analysis                                 | 236 |
| 4.9.2 | Optical Band Gap Energy   | 238 |
| 4.9.3 | Refractive Index  | 243 |
| 4.9.4 | Electronic Polarizability   | 244 |
| 4.9.5 | Emission Cross-Section  | 245 |
| 4.10  | Summary   | 248 |

 05-4506832
  [pustaka.upsi.edu.my](http://pustaka.upsi.edu.my)
 Perpustakaan Tuanku Bainun  
Kampus Sultan Abdul Jalil Shah
  PustakaTBainun
  ptbupsi

**CHAPTER 5 CONCLUSION AND RECOMMENDATION**

|     |                            |     |
|-----|----------------------------|-----|
| 5.1 | Introduction               | 249 |
| 5.2 | Conclusion                 | 250 |
| 5.3 | Future Work Recommendation | 254 |

|                   |     |
|-------------------|-----|
| <b>REFERENCES</b> | 257 |
|-------------------|-----|

|                   |     |
|-------------------|-----|
| <b>APPENDICES</b> | 285 |
|-------------------|-----|



## LIST OF TABLES

| Table No. |   | Page |
|-----------|---|------|
| 1.1       | Phonon energy of different glass hosts  | 5    |
| 1.2       | Comparing tellurite, silica, fluoride, and chalcogenide glasses.                  | 6    |
| 1.3       | Summary of the research problems and research solutions that relate to the study  | 13   |
| 2.1       | Comparison of glass and ceramics  | 20   |
| 2.2       | Glass definition  | 21   |
| 2.3       | Glass preparation at various techniques   | 25   |
| 2.4       | Deposition of various graphene-based materials                                    | 44   |
| 2.5       | Summary findings of the XRD analysis for various glass                            | 64   |
| 2.6       | The summary of assignment from FTIR spectra for RE doped zinc borotellurite glass | 69   |
| 2.7       | Summarization of previous studies on tellurite based glass                        | 99   |
| 3.1       | Weight of each chemical composition in the fabricated glasses                     | 105  |
| 3.2       | Raw materials to synthesis GO   | 109  |
| 4.1       | Density and molar volume of ZBTNd (NPs)-uncoated) glasses                         | 126  |





|      |  |     |
|------|--|-----|
| 4.2  | Oxygen packing density (OPD) value of ZBTNd (NPs)-uncoated glasses   | 128 |
| 4.3  | Neodymium ionic concentration (N), Inter-ionic distance (Ri), Polaron radius (Rp) of ZBTNd (NPs)- uncoated glasses   | 130 |
| 4.4  | Assignment of infrared transmission band of ZBTNd (NPs)-uncoated glasses   | 134 |
| 4.5  | Element of GO with Atomic percentage % and weight percentage %   | 143 |
| 4.6  | Optical band gap, for ZBTNd (NPs)-GO and ZBTNd-uncoated glasses  | 154 |
| 4.7  | Fermi energy of ZBTNd (NPs)-GO glasses and ZBTNd (NPs)-uncoated glasses  | 156 |
| 4.8  | Urbach energy of ZBTNd (NPs) uncoated and ZBTNd (NPs)-GO glasses   | 158 |
| 4.9  | Refractive index of ZBTNd (NPs)- uncoated and ZBTNd (NPs)-GO glasses   | 160 |
| 4.10 | Transmission coefficient (T), Reflection loss (RL), and Dielectric constant ( $\epsilon$ ) of ZBTNd (NPs)-GO glasses | 162 |
| 4.11 | Nephelauxetic ratio of ZBTNd (NPs)-GO glasses. Notes: Vc (from data experiment) Aquo from (Carnall et al., 1968)     | 164 |
| 4.12 | Optical Electronegativity of ZBTNd (NPs)-GO glasses  | 165 |
| 4.13 | Electronic polarizability of ZBTNd (NPs)-GO glasses  | 167 |
| 4.14 | Oxide ion polarizability of ZBTNd (NPs)-GO and ZBTNd (NPs)-uncoated glasses  | 170 |
| 4.15 | Optical basicity of ZBTNd (NPs)-uncoated and ZBTNd (NPs)-GO glasses  | 172 |
| 4.16 | Metallization criterion of ZBTNd (NPs)-uncoated and ZBTNd (NPs)-GO glasses   | 174 |
| 4.17 | Absorption cross-section and emission cross-section of ZBTNd (NPs)-GO glasses at 1600 nm wavelength                  | 179 |





|      |  |     |
|------|--|-----|
| 4.18 | Absorption cross-section and emission cross-section of ZBTNd (NPs)-GO glasses at 2500 nm wavelength  | 184 |
| 4.19 | Gain coefficient for ZBTNd (NPs)-GO glasses at 1400 -2000 nm wavelength  | 187 |
| 4.20 | Gain coefficient of ZBTNd (NPs)-GO glasses at 2000-2800 nm wavelength  | 191 |
| 4.21 | Element of rGO with Atomic percentage % and weight percentage %  | 195 |
| 4.22 | Optical band gap, energy for ZBTNd-uncoated and ZBTNd (NPs)-rGO glasses  | 205 |
| 4.23 | Fermi energy for ZBTNd-uncoated and ZBTNd (NPs)-rGO glasses  | 206 |
| 4.24 | Urbach energy for ZBTNd-uncoated and ZBTNd (NPs)-GO glasses  | 207 |
| 4.25 | Refractive index for ZBTNd-uncoated and ZBTNd (NPs)-rGO glasses  | 210 |
| 4.26 | Transmission coefficient (T), Reflection loss (RL), and Dielectric constant $\epsilon$ , of ZBTNd (NPs)-rGO glasses  | 211 |
| 4.27 | Nephelauxetic ratio of ZBTNd (NPs)-rGO glasses   | 212 |
| 4.28 | Optical Electronegativity of ZBTNd (NPs)-rGO glasses   | 214 |
| 4.29 | Electronic polarizability of ZBTNd (NPs)-rGO glasses   | 216 |
| 4.30 | Oxide ion polarizability of ZBTNd (NPs)-rGO glasses  | 218 |
| 4.31 | Optical basicity of ZBTNd (NPs)-rGO glasses  | 219 |
| 4.32 | Metallization criterion of ZBTNd (NPs)-uncoated and ZBTNd (NPs)-rGO glasses  | 221 |
| 4.33 | Absorption cross section-section ( $\sigma_{\text{abs}}$ ), emission cross-sections ( $\sigma_{\text{emis}}$ ) of ZBTNd NPs-rGO glasses at peak 1600 nm wavelength | 225 |





|      |   |     |
|------|---|-----|
| 4.34 | Absorption cross-section and emission cross-section of ZBTNd (NPS)-rGO glasses at 2500 nm wavelength. | 229 |
| 4.35 | Gain coefficient of ZBTNd (NPs)-rGO glasses   | 232 |
| 4.36 | Amount of chemical atomic % of graphene oxide (GO) and reduced graphene oxide (rGO)                   | 237 |
| 4.37 | Linear optical properties of ZBTNd (NPs)-GO and ZBTNd (NPs)-rGO glasses                               | 239 |
| 4.38 | Comparative value of optical properties neodymium doped glasses from previous studies.                | 241 |
| 4.39 | Emission cross –section at NIR emission for tellurite glass systems and previous literature           | 247 |





## LIST OF FIGURES

| No. Figures |   | Page |
|-------------|---|------|
| 1.1         | Overview of the research studies  | 2    |
| 1.2         | Application of GO and derivatives. Adapted from Dideikin & Vul', 2019   | 10   |
| 2.1         | The basic structure of commercial glass. Adapted from Shioya & Kikutani 2015  | 24   |
| 2.2         | Graphic representation of the melt-quenching method's preparatory phases for glass. Adapted from Karmakar, 2016   | 27   |
| 2.3         | The apparatus for glass preparation. Adapted from Sidek, 2011   | 29   |
| 2.4         | Tellurite glass structural units: (a) trigonal bipyramidal $\text{TeO}_4$ , (b) distorted trigonal bipyramidal $\text{TeO}_{3+1}$ , and (c) trigonal pyramidal $\text{TeO}_3$ . Dots show electrons that don't form bonds. Bond durations (in nm). Adapted from Burger et al., 1992 | 32   |
| 2.5         | Four types of structural groups in borate glasses: a) boroxol, b) pentaborate, c) triborate, and d) diborate. Adapted from Krogh-Moe, 1959  | 34   |
| 2.6         | Type of graphene production. Adapted from Hernaez et al., 2017  | 40   |
| 2.7         | Graphene oxide chemical structure. Adapted from Marcano et al., 2010  | 42   |
| 2.8         | Various of morphology of graphene oxide (GO) using FESEM instrument. Adapted from the literature (Azlina et al., 2020);(Azlina et al., 2021);(Saleem,   | 46   |





|      |   |    |
|------|---|----|
|      | Haneef & Abbasi, 2018);(Md Disa, 2017);(Muqoyyanah, 2019)   |    |
| 2.9  | Various of morphology of reduced graphene oxide (rGO) using FESEM instrument. Adapted from the literature (Azlina et al., 2020);(Azlina et al., 2021);(Saleem, Haneef & Abbasi, 2018);(Md Disa, 2017)                                 | 47 |
| 2.10 | EDX spectra and element content of the (a)-(c) graphene oxide (GO) and (b) reduced graphene oxide (rGO) synthesis from electrochemical exfoliation method using different surfactant. Adapted from Md Disa. 2017 and Muqoyyanah, 2019 | 48 |
| 2.11 | Example Raman spectra for GO and rGO. Adapted from Wu & Ting, 2013 and Azlina et al., 2022  | 50 |
| 2.12 | Several of XRD pattern using X-Ray Diffraction instrument. Adapted from literature (a) (Hamza et al., 2019); (b)(Jan et al., 2019); (c) (Abdulbaset et al., 2017)   | 63 |
| 2.13 | FTIR spectra zinc borotellurite glass doped with dysprosium oxide. Adapted from Halimah et al., 2018  | 66 |
| 2.14 | FTIR spectra of prepared glass sample with different concentration of lanthanum oxide. Adapted from Faznny et al., 2016   | 68 |
| 2.15 | TEM of erbium nanoparticles doped bio-silica borotellurite glasses. Adapted from Halimah et al., 2019   | 71 |
| 2.16 | Absorption spectra $\text{Nd}^{3+}$ ions doped $\text{TeO}_2\text{-ZnO-Na}_2\text{O}$ tellurite glasses. Adapted from Seshadri et al., 2018   | 75 |
| 2.17 | The absorption bands of $\text{Nd}^{3+}$ - doped zinc tellurite based glass. Adapted from Kesavulu et al., 2017   | 76 |
| 2.18 | Diagram of mechanism of electron moves from the valence band to the conduction band. Adapted from Abdel-Baki and El-Diasty, 2006  | 78 |





|      |  |     |
|------|--|-----|
| 2.19 | The flowchart of literature review of present in this study  | 102 |
| 3.1  | Overview flowchart of the research methodology in this study   | 104 |
| 3.2  | Flow diagram of glass fabrication preparation  | 107 |
| 3.3  | Experiment setting for graphene oxide (GO) synthesis via electrochemical exfoliation method.   | 108 |
| 3.4  | Reduction method of GO to reduced graphene oxide. (a)The schematic diagram and (b-c) Reduction process of SDS-GO using hydrazine hydrates                        | 110 |
| 3.5  | Deposition process. (a) Schematic diagram and spraying coating method on glasses samples, (b) Annealing process ,(c) A series glass sample after coating process | 111 |
| 3.6  | A fundamental component in X-ray diffraction. Adapted from Shaari, 2018  | 113 |
| 3.7  | FTIR NEXUS Thermo 69000 Nicolet instrument was used to analyse the structural bonding of glass network forming.  | 115 |
| 3.8  | Scanning Electron Microscopy Instrument (HITACHI model SU 8020) was investigate the microstructure surface onto the GO-coated and rGO – coated glasses           | 117 |
| 3.9  | ThermoScientific (DXR2XI) Confocal Micro Raman Imaging spectroscopy to identify the nature of defect in GO and rGO samples                                       | 118 |
| 3.10 | Energy Dispersive X-ray (EDX) Oxford X-MAX to detecting element in GO and rGO samples  | 119 |
| 3.11 | UV-Visible-NIR Perkin Elmer Lamda 950 instrument to analyse the optical absorption spectra of GO-coated and rGO-coated tellurite glass sample                    | 120 |
| 3.12 | a) Glass sample was mounted at sample mounting. b) analysed the sample according to the desired wavelength by using the UV-Visible-NIR instrument                | 121 |





|      |   |     |
|------|---|-----|
| 4.1  | Density and molar volume versus concentration of ZBTNd (NPs)-uncoated glasses   | 126 |
| 4.2  | Oxygen packing density (OPD) versus concentration of ZBTNd (NPs) uncoated glasses   | 127 |
| 4.3  | Neodymium ionic concentration (N) versus molar fraction of neodymium nanoparticles  | 129 |
| 4.4  | Inter-ionic distance ( $R_i$ ), Polaron radius ( $R_p$ ) of glass system versus molar fraction of neodymium nanoparticles     | 130 |
| 4.5  | FTIR spectra of ZBTNd (NPs)- uncoated glasses   | 133 |
| 4.6  | TEM morphology existing of neodymium NPs structure  | 135 |
| 4.7  | XRD pattern of ZBTNd (NPs)-uncoated   | 137 |
| 4.8  | Fold up layer of FESEM images of GO nanosheets onto the tellurite glass surfaces at 50K magnification                         | 139 |
| 4.9  | Large agglomerated FESEM images of GO nanosheets onto the tellurite glass surfaces at 30K magnification                       | 139 |
| 4.10 | Inhomogeneous distribution of FESEM images of GO nanosheets onto the tellurite glass surfaces at 10K magnification            | 140 |
| 4.11 | Layer and large agglomerate of FESEM images of GO nanosheets onto the tellurite glass surfaces at 50K magnification           | 140 |
| 4.12 | EDX spectra of GO   | 142 |
| 4.13 | EDX elemental mapping of (a) Carbon (C), (b) Oxygen (O), (c) Nitrogen (N), (d) Sulphur (S), (e) Natrium (Na) in the GO sample | 143 |
| 4.14 | Micro-Raman spectra of GO with inset morphology image at 50 $\mu\text{m}$   | 145 |





|      |   |     |
|------|---|-----|
| 4.15 | Absorption spectra of ZBTNd (NPs)-uncoated glasses  | 148 |
| 4.16 | Absorption spectra of ZBTNd (NPs)-GO glasses  | 150 |
| 4.17 | Extinction coefficient $k$ , versus wavelength nm of ZBTNd (NPs)-GO glasses   | 151 |
| 4.18 | $\alpha\hbar\omega)^{1/2}$ versus photon energy, $\hbar\omega$ (eV) versus photon energy, $\hbar\omega$ (eV) for ZBTNd (NPs)-GO glasses             | 153 |
| 4.19 | Optical bandgap variation values for ZBTNd (NPs)-GO and ZBTNd (NPs)-uncoated glasses  | 153 |
| 4.20 | Urbach Energy of ZBTNd (NPs)-GO glasses   | 157 |
| 4.21 | Refractive index versus concentration of ZBTNd NPs-uncoated and ZBTNd NPs-GO glasses  | 159 |
| 4.22 | Transmission coefficient and reflection loss variation with $\text{Nd}_2\text{O}_3$ (NPs) concentration for ZBTNd (NPs)-GO glasses                  | 162 |
| 4.23 | Optical electronegativity of ZBTNd (NPs)-GO glasses   | 165 |
| 4.24 | Electronic polarizability versus concentration for ZBTNd (NPs)-GO glasses   | 167 |
| 4.25 | Correlation of refractive index and electronic polarizability versus $\text{Nd}_2\text{O}_3$ nanoparticles concentration for ZBTNd (NPs)-GO glasses | 168 |
| 4.26 | Oxide ion polarizability versus $\text{Nd}_2\text{O}_3$ nanoparticles concentration of ZBTNd (NPs)-uncoated and ZBTNd (NPs)-GO                      | 170 |
| 4.27 | Optical basicity versus $\text{Nd}_2\text{O}_3$ nanoparticles concentration of ZBTNd (NPs)-uncoated and ZBTNd (NPs)-GO                              | 172 |
| 4.28 | Metallization criterion versus $\text{Nd}_2\text{O}_3$ nanoparticles concentration of ZBTNd (NPs)-uncoated and ZBTNd (NPs)-GO glasses               | 174 |





|      |  |     |
|------|--|-----|
| 4.29 | Absorption cross and emission cross-section spectra of $^4F_{3/2} \rightarrow ^4I_{15/2}$ transition for 0.01 mol Nd (NPs) for ZBTNd (NPs)-GO glasses                    | 176 |
| 4.30 | Absorption cross spectra of $^4F_{3/2} \rightarrow ^4I_{15/2}$ transition for 0.02 mol Nd (NPs) for ZBTNd (NPs)-GO glasses   | 176 |
| 4.31 | Absorption cross-section and emission cross-section spectra of $^4F_{3/2} \rightarrow ^4I_{15/2}$ transition for 0.03 mol Nd (NPs) for ZBTNd (NPs)-GO glasses            | 177 |
| 4.32 | Absorption cross-section and emission cross-section spectra of $^4F_{3/2} \rightarrow ^4I_{15/2}$ transition for 0.04 mol Nd (NPs) for ZBTNd (NPs)-GO glasses            | 178 |
| 4.33 | Absorption and emission cross-section spectra of $^4F_{3/2} \rightarrow ^4I_{15/2}$ transition for 0.05 mol Nd <sub>2</sub> O <sub>3</sub> (NPs) for GO (ZBTNd (NPs)-GO) | 179 |
| 4.34 | Absorption cross-section and emission cross-section spectra of $^4F_{3/2} \rightarrow ^4I_{13/2}$ transition for 0.01 mol Nd (NPs) for ZBTNd (NPs)-GO glasses            | 180 |
| 4.35 | Absorption cross-section and emission cross-section spectra of $^4F_{3/2} \rightarrow ^4I_{13/2}$ transition for 0.02 mol Nd (NPs) for ZBTNd (NPs)-GO glasses            | 181 |
| 4.36 | Absorption cross-section and emission cross-section spectra of $^4F_{3/2} \rightarrow ^4I_{13/2}$ transition for 0.03 mol Nd (NPs) for ZBTNd (NPs)-GO glasses            | 182 |
| 4.37 | Absorption cross-section and emission cross-section spectra of $^4F_{3/2} \rightarrow ^4I_{13/2}$ transition for 0.04 mol Nd (NPs) for ZBTNd (NPs)-GO glasses            | 182 |
| 4.38 | Absorption cross and emission cross-section spectra of $^4F_{3/2} \rightarrow ^4I_{13/2}$ transition for 0.05 mol Nd (NPS) for ZBTNd (NPs)-GO glasses                    | 183 |
| 4.39 | Gain coefficient versus wavelength at 1400-2000 nm for 0.01 mol Nd (NPs) of ZBTNd (NPs)-GO glasses   | 185 |
| 4.40 | Gain coefficient versus wavelength at 1400-2000 nm for 0.02 mol Nd (NPs) of ZBTNd (NPs)-GO glasses   | 185 |





|      |  |     |
|------|--|-----|
| 4.41 | Gain coefficient versus wavelength at 1400-2000 nm for 0.03 mol Nd (NPs) of ZBTNd (NPs)-GO glasses                             | 186 |
| 4.42 | Gain coefficient versus wavelength at 1400-2000 nm for 0.04 mol Nd (NPs) of ZBTNd (NPs)-GO glasses                             | 186 |
| 4.43 | Gain coefficient versus wavelength at 1400-2000 nm for 0.05 mol Nd (NPs) of ZBTNd (NPs)-GO glasses                             | 187 |
| 4.44 | Gain coefficient versus wavelength at 2000-2800 nm for 0.01 mol Nd (NPs) of ZBTNd (NPs)-GO glasses                             | 188 |
| 4.45 | Gain coefficient versus wavelength at 2000-2800 nm for 0.02 mol Nd (NPs) of ZBTNd (NPs)-GO glasses                             | 189 |
| 4.46 | Gain coefficient versus wavelength at 2000-2800 nm for 0.03mol Nd (NPs) of ZBTNd (NPs)-GO glasses                              | 189 |
| 4.47 | Gain coefficient versus wavelength at 2000-2800 nm for 0.04mol Nd (NPs) of ZBTNd (NPs)-GO glasses                              | 190 |
| 4.48 | Gain coefficient versus wavelength at 2000-2800 nm for 0.05 mol Nd (NPs) of ZBTNd (NPs)-GO glasses                             | 190 |
| 4.49 | Exfoliated and staked rGO FESEM images onto the tellurite glass surfaces at 10K magnification                                  | 192 |
| 4.50 | Folder up multiple layers and stacked rGO FESEM images onto the tellurite glass surfaces at 20K magnification.                 | 192 |
| 4.51 | Uneven and irregular distribution FESEM images of rGO onto the tellurite glass surfaces at 20K magnification                   | 193 |
| 4.52 | Uneven and irregular distribution FESEM images of rGO onto the tellurite glass surfaces at 10K magnification.                  | 193 |
| 4.53 | EDX spectra of rGO solution  | 195 |
| 4.54 | EDX elemental mapping of (a) Carbon (C), (b) Nitrogen (c) Sulphur (S), (d) Oxygen (O), (N), (e) Natrium (Na) in the rGO sample | 196 |





|      |  |     |
|------|--|-----|
| 4.55 | Micro-Raman spectra of GO with inset morphology image at 50 $\mu\text{m}$ spectra of rGO   | 197 |
| 4.56 | Absorption spectra of ZBTNd (NPs)-uncoated glasses   | 199 |
| 4.57 | Absorption spectra of ZBTNd (NPs)-rGO glasses  | 200 |
| 4.58 | Extinction coefficient, $k$ versus wavelength nm of tellurite glass doped neodymium nanoparticles (ZBTNd (NPs)-rGO)                                  | 202 |
| 4.59 | $(\alpha\hbar\omega)^{1/2}$ versus photon energy, $\hbar\omega$ (eV) versus photon energy, $\hbar\omega$ (eV) for ZBTNd (NPs)-rGO glasses            | 203 |
| 4.60 | Optical bandgap variation values for ZBTNd (NPs)-uncoated and ZBTNd (NPs)-rGO  | 204 |
| 4.61 | Urbach Energy of ZBTNd (NPs)-rGO glasses   | 207 |
| 4.62 | Refractive index versus $\text{Nd}_2\text{O}_3$ nanoparticles concentration of ZBTNd (NPs)-uncoated glasses and ZBTNd (NPs)-rGO glasses              | 209 |
| 4.63 | Reflection loss, transmission coefficient versus neodymium molar fraction of ZBTNd (NPs)-rGO glasses   | 211 |
| 4.64 | Optical Electronegativity of ZBTNd (NPs)-rGO glasses   | 214 |
| 4.65 | Electronic polarizability versus concentration of ZBTNd (NPs)-rGO glasses  | 215 |
| 4.66 | Correlation of electronic polarizability and refractive index versus $\text{Nd}_2\text{O}_3$ nanoparticles concentration for ZBTNd (NPs)-rGO glasses | 216 |
| 4.67 | Oxide ion polarizability versus molar fraction neodymium nanoparticles of ZBTNd (NPs)-rGO glasses  | 217 |
| 4.68 | Optical basicity versus concentration of $\text{Nd}_2\text{O}_3$ NPS for ZBTNd (NPs)-rGO glasses   | 219 |





|      |  |     |
|------|--|-----|
| 4.69 | Metallization criterion versus concentration of ZBTNd (NPs)-rGO glasses  | 220 |
| 4.70 | Absorption cross-section and emission cross-section spectra of $^4F_{3/2} \rightarrow ^4I_{15/2}$ transition for 0.01 mol Nd (NPs) for ZBTNd (NPs)-rGO glasses | 222 |
| 4.71 | Absorption cross-section and emission cross-section spectra of $^4F_{3/2} \rightarrow ^4I_{15/2}$ transition for 0.02 mol Nd (NPs) for ZBTNd (NPs)-rGO glasses | 223 |
| 4.72 | Absorption cross-section and emission cross-section spectra of $^4F_{3/2} \rightarrow ^4I_{15/2}$ transition for 0.03 mol Nd (NPs) for ZBTNd (NPs)-rGO glasses | 223 |
| 4.73 | Absorption cross-section and emission cross-section spectra of $^4F_{3/2} \rightarrow ^4I_{15/2}$ transition for 0.04 mol Nd (NPs) for ZBTNd (NPs)-rGO glasses | 224 |
| 4.74 | Absorption cross-section and emission cross-section spectra of $^4F_{3/2} \rightarrow ^4I_{15/2}$ transition for 0.05 mol Nd (NPs) for ZBTNd (NPs)-rGO glasses | 224 |
| 4.75 | Absorption cross-section and emission cross-section of $^4F_{3/2} \rightarrow ^4I_{13/2}$ transition for 0.01 mol Nd (NPS) of ZBTNd (NPs)-rGO glasses          | 226 |
| 4.76 | Absorption and emission cross-section of $^4F_{3/2} \rightarrow ^4I_{13/2}$ transition for 0.02 mol Nd (NPS) of ZBTNd (NPs)-rGO glasses                        | 226 |
| 4.77 | Absorption cross-section and emission cross-section of $^4F_{3/2} \rightarrow ^4I_{13/2}$ transition for 0.03 mol Nd (NPS) of ZBTNd (NPs)-rGO glasses          | 227 |
| 4.78 | Absorption cross-section and emission cross-section of $^4F_{3/2} \rightarrow ^4I_{13/2}$ transition for 0.04 mol Nd (NPS) of ZBTNd (NPs)-rGO glasses          | 228 |
| 4.79 | Absorption and emission cross-section of $^4F_{3/2} \rightarrow ^4I_{13/2}$ transition for 0.05 mol Nd (NPS) of ZBTNd (NPs)-rGO glasses                        | 228 |
| 4.80 | Gain coefficient versus wavelength at 1400-2000 nm for 0.01 mol Nd (NPs) for ZBTNd (NPs)-rGO glasses   | 230 |





|      |  |     |
|------|--|-----|
| 4.81 | Gain coefficient versus wavelength at 1400-2000 nm for 0.02 mol Nd (NPs) for ZBTNd (NPs)-rGO glasses                           | 231 |
| 4.82 | Gain coefficient versus wavelength at 1400-2000 nm for 0.03 mol Nd (NPs) for ZBTNd (NPs)-rGO glasses                           | 231 |
| 4.83 | Gain coefficient versus wavelength at 1400-2000 nm for 0.04 mol Nd (NPs) for ZBTNd (NPs)-rGO glasses                           | 232 |
| 4.84 | Gain coefficient versus wavelength at 1400-2000 nm for 0.05 mol Nd (NPs) for ZBTNd (NPs)-rGO glasses                           | 232 |
| 4.85 | Gain coefficient versus wavelength at 2200-2800 nm for 0.01 mol Nd (NPs) for ZBTNd (NPs)-rGO glasses                           | 233 |
| 4.86 | Gain coefficient versus wavelength at 2200-2800 nm for 0.02 mol Nd (NPs) for ZBTNd (NPs)-rGO glasses                           | 233 |
| 4.87 | Gain coefficient versus wavelength at 2200-2800 nm for 0.03 mol Nd (NPs) for ZBTNd (NPs)-rGO glasses                           | 234 |
| 4.88 | Gain coefficient versus wavelength at 2200-2800 nm for 0.04 mol Nd (NPs) for ZBTNd (NPs)-rGO glasses                           | 234 |
| 4.89 | Gain coefficient versus wavelength at 2200-2800 nm for 0.05 mol Nd (NPs) for ZBTNd (NPs)-rGO glasses                           | 235 |
| 4.90 | Comparison of a (a) FESEM image of GO at 20K magnification and (b) FESEM image of rGO at 10K magnification                     | 237 |
| 4.91 | A graph showing comparison between the optical energy bandgap of ZBTNd (NPs)-GO and ZBTNd (NPs)-rGO tellurite glass system     | 239 |
| 4.92 | A graph showing comparison between the refractive index of ZBTNd (NPs)-GO and ZBTNd (NPs)-rGO tellurite glass system           | 244 |
| 4.93 | A graph showing comparison between the electronic polarizability of ZBTNd (NPs)-GO and ZBTNd (NPs)-rGO tellurite glass system. | 245 |





## LIST OF ABBREVIATION

|                               |  |                   |
|-------------------------------|--|-------------------|
| $\Delta E$                    | Energy   | joule (J)         |
| $\Delta E_u$                  | Urbach Energy                                  | Joule (J)/eV      |
| $\Delta E_u$                  | Urbach Energy                                  | Joule (J)/eV      |
| A                             | Area   | m <sup>2</sup>    |
| Ag                            | silver   | -                 |
| Au                            | gold   | -                 |
| B <sub>2</sub> O <sub>3</sub> | Borate oxide                                   | -                 |
| BO                            | bridging oxygen                                | -                 |
| d                             | Thickness                                      | m                 |
| EDX                           | Energy Dispersive X-ray                        | -                 |
| E <sub>opt</sub>              | Optical energy gap                             | Joule (J)/eV      |
| FESEM                         | Field Emission Scanning Electron<br>Microscope | -                 |
| FTIR                          | Fourier Transform Infrared                     | -                 |
| GO                            | Graphene Oxide                                 | -                 |
| K <sub>B</sub>                | Boltzmann constant                             | -                 |
| M                             | Metallization criterion                        | -                 |
| n                             | Refractive index                               | -                 |
| N <sub>A</sub>                | Avogadro number                                | mol <sup>-1</sup> |





|                                |   |                     |
|--------------------------------|---|---------------------|
| NBO                            | Non Bridging Oxygen   | -                   |
| Nd <sub>2</sub> O <sub>3</sub> | Neodymium oxide   | -                   |
| Nd <sup>3+</sup>               | Neodymium Ion   | -                   |
| Nps                            | Nanoparticles   | -                   |
| RE                             | Rare-earth  | -                   |
| REIs                           | Rare-earth ions   | -                   |
| rGO                            | Reduced Graphene Oxide (rGO)  | -                   |
| T                              | Temperature   | degree celcius      |
| TEM                            | Transmission Electron Microscopy  | -                   |
| TeO <sub>3</sub>               | Trigonal Pyramid  | -                   |
| TeO <sub>4</sub>               | Trigonal Bipyramid  | -                   |
| V <sub>m</sub>                 | Molar volume  | m <sup>3</sup> /mol |
| XRD                            | X-Ray Diffraction   | -                   |
| ZBTNd (NPs)                    | Neodymium Nanoparticles Doped Zincborotellurite                               |                     |
| ZBTNd (NPs)-GO                 | Graphene Oxide Coated Neodymium Nanoparticles Doped Zincborotellurite         |                     |
| ZBTNd (NPs)-rGO                | Reduced Graphene Oxide Coated Neodymium Nanoparticles Doped Zincborotellurite |                     |
| ZnO                            | Zinc Oxide  |                     |
| $\alpha_e$                     | Electronic Polarizability   | Å <sup>3</sup>      |
| $\alpha_o^{2-}$                | Oxide Ion Polarizability  | Å <sup>3</sup>      |
| $\beta$                        | Nephelauxetic ratio   | -                   |





|               |                        |                   |
|---------------|------------------------|-------------------|
| $\delta$      | Bonding parameter      | -                 |
| $\Lambda$     | Optical basicity       | -                 |
| $\lambda$     | Wavelength             | m                 |
| $\rho$        | Density                | kg/m <sup>3</sup> |
| $\nu_a$       | Wavenumber aquo-ion    | cm <sup>-1</sup>  |
| $\nu_c$       | Wavenumber host matrix | cm <sup>-1</sup>  |
| $\omega$      | Radian Frequency       | Fm <sup>-1</sup>  |
| $\hbar\omega$ | Photon energy          | Joule (J)/eV      |



## LIST OF APPENDICES

- A Academic Journal
- B Presentation
- C Awards
- D The Synthesis of Graphene Oxide

## CHAPTER 1

### INTRODUCTION

#### 1.1 Introduction

This chapter describes a brief introduction to the research background, research problems and objectives. The significance of the studies, scopes and limitations of the study are presented in this chapter. In addition, the explanation overview of the research work is presented in Figure 1.1. The last part of this chapter ended with a summary of the thesis outline.

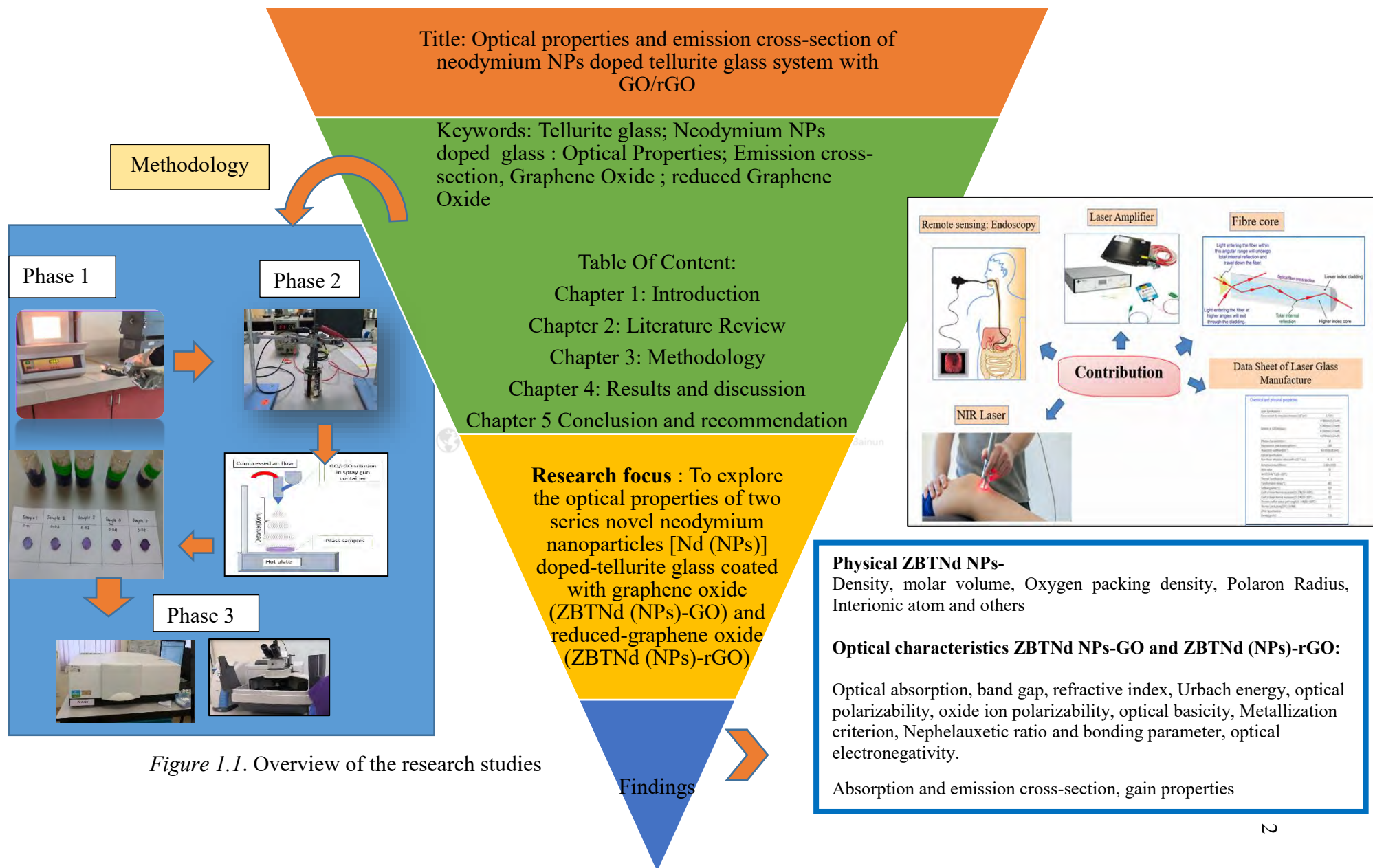


Figure 1.1. Overview of the research studies

## 1.2 Research Background

Glass is a multipurpose material that is used frequently in many applications. Glass can be a stiff, brittle, and transparent solid. This characteristic demonstrates that glass has exceptional qualities for technological and decorative applications. Furthermore, glass has the advantages of being recyclable, chemically resistant, and durable in a wide range of temperatures. These characteristics demonstrate the importance of glass in technological applications, including architecture, packaging, glassware, photovoltaics, and the most cutting-edge fields of microelectronics and photonics (Sidek, 2011).

In the context of photonics applications, particularly telecommunications and laser applications, advanced glass materials are used to manufacture glass optical fibres and optical components (Righini, 2022). Thus, further research is required to produce optical fibre glass materials that can transmit more signals in telecommunications systems and serve as fibre and laser amplifiers (Azlan, 2016). Some researchers, for instance, have enhanced the performance of existing glass by incorporating rare earth elements such as erbium, ytterbium, neodymium, thulium, samarium, gadolinium and others (Kaewkhao et al., 2022; Manzani et al., 2012; Su et al., 2018; Tafida et al., 2023; Eevon et al., 2016) particularly those pertaining to its structure and optical quality. In order to avoid issues such as high production, instability in glass properties, and the tendency for glass to break, it is crucial to minimise defects during glass production (Azlan et al., 2019). Furthermore, replacing existing glass optical materials necessitates the selection of glass materials with superior optical quality and exceptional stability. Thus, several drawbacks must be

overcome to manufacture better optical materials for glass fibre optics and laser technology.

According to El-Mallawany (2011), tellurite glasses have scientific and technological significance due to their physical and optical properties. Tellurite oxide is the most stable oxide and its properties inspired scientists to conduct research. This substance possesses chemical resistance, a higher normal index, thermal resistance, and non-hygroscopic properties (Pandarinath et al., 2016). Moreover, tellurite-based glass possesses a high third-order nonlinear susceptibility, making it suitable for use in optical amplifiers (Gayathri Pavani et al., 2011). In addition, tellurite glass has a lower phonon energy than host glasses containing borate, phosphate, silicate, and germanate. Table 1.1 lists the categories of glass and their respective phonon energies. According to Tarafdeer et al., (2016) glass with a high phonon energy would show weak optical absorption cross sections, large non-radiative energy loss, and reduced upconversion luminescence performance. Table 1.2 compares the tellurite in chalcogenide, fluoride, and silica glasses. The exceptional optical and physical characteristics of tellurite-based glass make it the ideal substrate for photonic applications (Wang et al., 1994).

Meanwhile, Stambouli et al., (2012) stated that tellurite glass is widely recognised to be a potential host for photonic glass owing to its exceptional stability with rare-earth (RE) ions, a wide-reaching radiation window, and its ability to function well as a laser host, among other things. This glass has a high refractive index of 2.0 and is chemically stable,

making it a superior choice compared to other glasses like borate, germinate, silicate, and phosphate glasses (Azlan et al., 2019; Sharma et al., 2022).

Table 1.1

*Phonon energy of different glass hosts*

| Glass hosts | Phonon Energy (cm <sup>-1</sup> ) |
|-------------|-----------------------------------|
| Borate      | 1400                              |
| Phosphate   | 1200                              |
| Silica      | 1100                              |
| Germanate   | 900                               |
| Tellurite   | 700                               |

Adapted from Tarafder et al., 2016

Table 1.2

*Comparing tellurite, silica, fluoride, and chalcogenide glasses.*

| Property   | Tellurite             | Silica                            | Fluoride                                 | Chalcogenide                   |
|--|-----------------------|-----------------------------------|--|--------------------------------|
| <i>Optical properties (typical values)</i>   |                       |                                   |  |                                |
| Refractive index ( $n$ )   | 1.8–2.3               | 1.46                              | 1.5                                      | 2.83                           |
| Abbe number ( $\nu$ )  | 10–20                 | 80                                | 60–110                                   |                                |
| Nonlinear refractive index ( $n_2$ , $\text{m}^2/\text{W}$ )                                 | $2.5 \times 10^{-19}$ | $10^{-20}$                        | $10^{-21}$                               | higher                         |
| Transmission range ( $\mu\text{m}$ )   | 0.4–5.0               | 0.2–2.5                           | 0.2–7.0                                  | 0.8–16                         |
| Highest phonon energy ( $\text{cm}^{-1}$ )   | 800                   | 1000                              | 500                                      | 300                            |
| Longest fluorescent wavelength ( $\mu\text{m}$ )   | 2.8                   | 2.2                               | 4.4                                      | 7.4                            |
| Bandgap (eV)   | $\approx 3$           | $\approx 10$                      |  | 1–3                            |
| Acousto-optical figure of merit,<br>$p^2 n^6 / \rho v^3$ ( $10^{-18} \text{ s}^3/\text{g}$ ) | 24                    | 1–19                              | –  |                                |
| <i>Physical properties (typical values)</i>  |                       |                                   |  |                                |
| Glass transition ( $T_g$ , $^\circ\text{C}$ )  | 300                   | 1000                              | 300                                      | 300                            |
| Thermal expansion ( $10^{-7} \text{ }^\circ\text{C}$ )                                       | 120–170               | 5                                 | 150                                      | 140                            |
| Density ( $\text{g}/\text{cm}^3$ )   | 5.5                   | 2.2                               | 5.0                                      | 4.51                           |
| Dielectric constant ( $\epsilon$ )   | 13–35                 | 4.0                               | –  |                                |
| Fiber loss   | –                     | 0.2 dB/km<br>(1.5 $\mu\text{m}$ ) | 15–25 dB/km<br>(1.5–2.75 $\mu\text{m}$ ) | 0.4 dB/km<br>6.5 $\mu\text{m}$ |
| Bonding  | covalent-ionic        | ionic-covalent                    | ionic                                    | covalent                       |
| Solubility in water  | $< 10^{-2}$           | $< 10^{-3}$                       | soluble                                  | $< 10^{-4}$                    |

Adapted from Wang et., al 1994



Ternary tellurite-based glass systems are stable due to the combination of the glass modifier and glass former. Due to its instability and propensity to crystallise, pure  $\text{TeO}_2$  cannot by itself produce glass (Azlan, 2016; Hasim, 2014).  $\text{TeO}_2$  must be modified with substances like alkali, alkali earth, and transition metal oxide to improve its capacity to form glass. In particular, the physical features, density, optical qualities, and mechanical durability of glass systems may change as a result of the inclusion of these modifiers (Effendy et al., 2021).

Tellurium oxide ( $\text{TeO}_2$ ), borate oxide and zinc oxide are regarded as the optimal choices for modifying tellurite-based glass systems. According to reports, incorporating borate into  $\text{TeO}_2$  glass increases infrared transmission and reduces hygroscopicity. (Azlan et al., 2017). Some researchers believe that  $\text{B}_2\text{O}_3$  is an exceptional glass-forming element because it can exist with three or four coordinates and produce stable glasses. It has tremendous potential as a novel optical device. Due to its highly soluble with rare-earth ions and strong B-O covalent bonds. Furthermore, incorporation of a small quantity of  $\text{TeO}_2$  to the borate glass matrix enhances both the transparency and refractive index of the glass, thereby augmenting its overall quality. (Ami Hazlin et al., 2017; Faznny et al., 2017; Gayathri Pavani et al., 2011; Halimah et al., 2020; Pandarinath et al., 2016).

In order to enhance the rigidity, chemical resistance, and thermodynamic properties development of glass systems, zinc oxide has been used as glass modifier. The inclusion of zinc oxide within the glass matrix reduces the crystallization rate. Zinc oxide may act as a network former or network modifier that may infiltrate the glass



structure. As a network modifier, ZnO causes the formation of non-bonding oxygens (NBOs) by breaking the Te-O-Te bond (Effendy et al., 2021).

Incorporating rare earth elements into different glass oxides plays a pivotal role in advancing of optical devices, including infrared lasers, visible conversion devices, and fibre and waveguide boosters, which are essential for applications in telecommunications networks. In addition, there is considerable interest in employing trivalent rare earth ions as functional components in glass host substances due to the presence of numerous fluorescent states with the 4f electron configuration, the majority of which are visible. These ions play a crucial role in facilitating rapid pumping applications and allowing dye lasers to be tuned (Hasim, 2014).

According to (Jha et al., 2012), the use of rare-earth doped tellurium oxide ( $\text{TeO}_2$ ) in glass lasers provides for more wavelength flexibility as well as superior Q-switching and mode-locking for power density at fewer pump energies as compared to crystal-based products. Neodymium oxide is among the superior rare-earth oxides utilised variety of devices that deal with optics including lasing materials, broadband amplifiers, and laser glass (Azlina et al., 2020). Because of the unique optical properties of the 4f shell, neodymium nanoparticles embedded in tellurite glass may offer a potential laser material to replace the present neodymium-doped phosphate laser glass (Halimah et al., 2020; Shaari et al., 2021).

Moreover, neodymium oxide in tellurite glass provides a minimal laser level of 8 mW and lowers losses within during the development of laser glass, (Azlan et al., 2019; Bell et al., 2014). Also, neodymium-doped tellurite is appropriate for optical

amplification or solid-state lasers, and it emits NIR light efficiently at 1062 nm (Venkateswarlu et al., 2015). Therefore, we will be doing this research using rare-earth neodymium nanoparticles as our active element material choice for the tellurite glass systems.

The use of graphene based materials has attracted the interest of researchers, notably in laser applications (Kant et al., 2022; Tseng et al., 2021; Wang et al., 2023) . Novoselov et al. stated in 2004 that graphene has several excellent properties, such as strong electrical conductivity, flexibility, and toughness (Novoselov et al., 2004). Moreover, graphene materials possess exceptional optical properties. However, graphene embedding into long stretches of fibre has limitations because of the difficulty of controlling graphene in particle form, which leads to transmission interruptions (Ruan et al., 2016; Shaari et al., 2022).

So, another graphene-based material derivative known as graphene oxide (GO) and reduced graphene oxide (rGO) has been used as a replacement of graphene flakes in the production of fibres for use in ultrafast laser and sensor applications, among other things. The remarkable characteristics of GO and derivatives have attracted the interest of many uses (Gerosa et al., 2020; Kavitha & Jaiswal, 2016), as shown in Figure 1.2, including optoelectronics, supercapacitors, or an energy storage device like lithium-ion rechargeable batteries based on graphene oxide, sensor (biosensor) solar cells, catalysts, photocatalysts, and more applications. (Azlina et al., 2021; Dideikin & Vul', 2019).

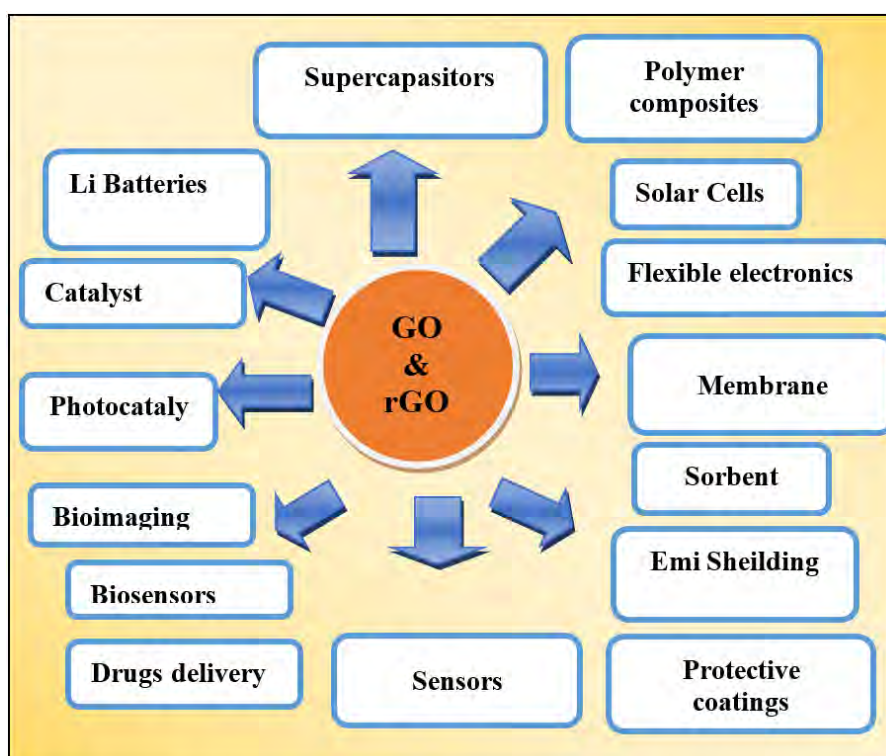


Figure 1.2. Application of GO and derivatives. Adapted from Dideikin & Vul', 2019

Graphene oxide comprises stacked layers with numerous oxygen functional groups, including epoxy, hydroxyl, carboxyl, and carbonyl groups. Azlina et al., (2020) observed that oxygen-containing functional groups in GO layers improved optical characteristics, indicating that GO significantly impacted tellurite glass for optical fibre (Azlina et al., 2020). Combining this graphene-based material with tellurite glass is yet another technique for increasing the optical properties of the glass network system. Graphene based materials is the most outstanding choice for making superb glass coatings and is highly advantageous to fibre optic applications. According to reports, the graphene-based material coating on the tellurite surface leads to the glass having a high refractive index of more than 2.000, ranging from 2.301 to 2.332 (GO) (Azlina et al., 2021) and 2.402 to 2.775 (rGO) (Azlina et al., 2023). Therefore, this technique can

improve superior fibre core materials, especially optical fibre, and will enhance optical fibre laser technology.






As an outcome result, a more comprehensive study into the utilization of graphene-based materials and optical glass materials is essential in order to enhance the optical properties of glass systems. Additionally, this innovative research can yield extremely intriguing outcomes, particularly for the fibre optic and fibre laser technology industries.

### 1.3 Research Problems

Neodymium-doped phosphate oxide glasses are commonly use as the host material for laser gain media in the fibre laser and laser glass industry due to their high solubility, large emission cross-section, and long lifetimes (He et al., 2017; MetaLaser, 2022a). However, phosphate oxide glass is limited in manufacturing the highest laser power at ambient conditions due to poor optical sensitivity (Deepa et al., 2019), low chemical stability (Elbakey et al., 2020), and high hygroscopic properties (Jan et al., 2019; Zaid et al., 2012). As a result, it has low strength, high fragility, and is prone to fracture (Hamzah et al., 2017), which can increase production costs and sensitivity to back-reflected light, leading to laser glass failure. Furthermore, it has been observed that phosphate glass exhibits a diminished stark splitting effect, leading to certain thermal drawbacks (Azlan et al., 2018). Zhang et al. reported that unsatisfactory lasing performance of  $\text{Yb}^{3+}$  phosphate glass resulting in narrow stark splitting where effect thermal block during laser operation (Zhang et al., 2015). To overcome this issue, new

glass materials with improved optical qualities must be invented to replace the current laser gain media materials. Therefore, tellurite glass is selected to replace the current host material due to of the low hygroscopic, high solubility of rare earth ions and the ease of drawing fibres at low temperatures compared with phosphate glass.

Tellurite glass is a very promising host glass for optical glass in these studies. Due to its exceptional qualities, including its excellent match with rare-earth (RE) ions. It has been chosen over other glass oxides due to its broad transmittance window, outstanding laser medium (Barbosa et al., 2017; Syam Prasad & Venkateswara Rao 2018), excellent laser host (Jha et al., 2012; Oermann, 2011), and good chemical resistance (Elkhoshkhany et al., 2021; Halimah et al., 2021).

 05-4506832
 pustaka.upsi.edu.my
 Perpustakaan Tuanku Bainun  
Kampus Sultan Abdul Jalil Shah
 PustakaTBainun
 ptbupsi

Recently, most researchers have been focusing their attention on a few techniques, such as co-doping the host glass with two different REIs and embedding optically effective NP-metallic (Au/Ag) or transition oxide. This approach is an improvement technique that can boost the optical performance of glass systems (Abdullahi et al., 2020; Halimah et al., 2021; Manzani et al., 2017; Peng et al., 2015; Saad, 2019; Yu et al., 2018; Dechun Zhou et al., 2017).

A carbon-based material coating is an additional method. Several studies suggested that deposition of GO, rGO and CNT films onto the surface of tellurite glass could improve the optical characteristics of laser glass (Azlina, 2023; Azlina et al., 2021; Azlina et al., 2020; Shaari et al., 2021). However, the application of carbon-based materials to optical fibre glass remains unestablished, lack of data in publication and requires additional research. Therefore, additional research must be conducted to

contribute new information to optical fibre and laser applications. Furthermore, the research on glass coating can be more extended to overcome these limitations. The deposition of carbon-based materials especially graphene oxide (GO) and reduced graphene oxide (rGO) coated on glass surface via a simple spray coating technique can be step to achieve high functionality of optical fibre especially in the application of fiber optics technology. In summary, the research proposed in the present study are summerized in Table 1.3.

Table 1.3

*Summary of the research problems and research solutions that relate to the study*

| Research Problem   | Research Solution   |
|--|---|
| Poor optical sensitivity, low chemical instability, and high hygroscopic properties (Hamzah et al., 2017), contribute to the high production cost of phosphate oxide glass.                      | Replace the new glass host materials, which are tellurite glass, with exceptional characteristics, particularly to improve the optical attributes of the existing glass host. |
| Enhancement of the properties of optical glass by using co-doping with two different REIs and embedding optically effective NP-metallic (Au/Ag) or transition oxide, which can lead to expensive | Utilising a glass coating approach with graphene-based materials on the glass improved the optical properties of the low-priced glass system.                                 |

(continue)

Table 1.3 (*continued*)

| Research Problem   | Research Solution  |
|--|--|
| production costs in glass fabrication<br><br>(Abdullahi et al., 2020; Halimah et al., 2021; Manzani et al., 2017; Peng et al., 2015; Saad, 2019; Yu et al., 2018; Dechun Zhou et al., 2017). |  |
| The previous researcher reported the lack of data on publications regarding the usage of carbon-based materials as coating materials for optical glass (Shaari et al., 2021).                | Expansion research on carbon-based material coating such as GO and rGO in optical glass may provide novel knowledge for fibre optics technology. |

## 1.4 Research Objectives

The purpose of this study is to examine the impact of deposited carbon-based materials, such as graphene oxide (GO) or reduced graphene oxide (rGO), on tellurite glass systems, with a particular focus on structural and optical property enhancements. Based on the purpose, the following are the objectives of this study are:

1. To study the surface morphology,particle size, and bonding parameter of ZBTNd (NPs) glasses, GO and rGO solution by using FESEM, FTIR, TEM, XRD and Raman Spectroscopy.

2. To analyze the absorption spectra, refractive index, optical band gap energy, Urbach energy, Fermi energy and the nephelauxetic ratio of ZBTNd (NPs)-GO and ZBTNd (NPS)-rGO glasses by using UV-Vis spectroscopy
3. To determine the electronic polarizability, oxide ion polarizability, optical basicity, and metallization criterion of ZBTNd (NPs)-GO and ZBTNd (NPs)-rGO the glasses via the Lorentz-Lorentz equation.
4. To investigate the stimulated emission cross-section and gain efficiency of ZBTNd (NPs)-GO and ZBTNd (NPs)-rGO glasses

### 1.5 Significance of the Study

The nanomaterial coating technique, which is also very important in nano-intermediate science, will result in significant scientific and technical advances (Cao et al., 2013). Graphene oxide (GO) and reduced graphene oxide (rGO) have been used on glass fibre to enhance their mechanical and electronic properties. According to Ruan et al., (2016) graphene oxide can be combined with glass fibre, which can excite light and capture signals from a distance, making it a perfect medium for a range of practical applications to utilise applications of its unique optical and electronic properties. It could also be used in many fields, especially as flexible conducting wires, multifunctional fibres, and sensitive sensors (Fang et al., 2019). Besides, the ability of GO and rGO also has been explored in past several years to improve the enhanced mechanical and electrical properties, especially on composites reinforced by short fibres (Bhanuprakash, Parasuram, & Varghese, 2019).

Moreover, the graphene oxide can improve the optical properties of tellurite glass samples, making them acceptable for use in applications involving fibre optics. Azlina et al., (2020) found that the graphene-based effect increased the values of optical band gap energy, refractive index, and electronic polarizability after deposit compared to uncoated glass. Thus, it is advantageous to reduce photon energy losses during the transmission process in fibre optics applications.

Thus, the purpose of this study is to investigate the structural and optical properties of carbon-based coated neodymium nanoparticle-doped tellurite glass, which has the potential to contribute to technological advancements in optical applications. In addition, the obtained data may be used to improve the capabilities of glass and raise its laser emission potential. In addition, theoretical and experimental findings may be investigated in these glass materials as potential near-infrared laser active media, as well as the effect of GO/rGO as a glass coating on the optical parameter of tellurite glass systems.

## 1.6 Scope and Limitation of the Study

Firstly, neodymium-doped zinc borotellurite glass system of  $\{(0.47(1-y)) \text{ TeO}_2 + (0.2(1-y)) \text{ B}_2\text{O}_3 + (0.29(1-y)) \text{ ZnO} + (y) \text{ Nd}_2\text{O}_3 \text{ (nanoparticles)}\}$  GO/rGO (coated), ( $y=0.01, 0.02, 0.03, 0.04$  and  $0.05$ ) molar fraction denoted as ZBTNd (NPs)-GO and ZBTNd (NPs)-rGO were fabricated by using conventional melt quenching method.

After the sample preparation, graphene oxide (GO) and reduced graphene oxide (rGO) will be synthesised using electrochemical exfoliation from the graphite electrode and the reduction process of GO. All the glass samples will be coated with GO/ rGO using the spraying method. Several analysis techniques were utilised for characterisation, such as UV-Visible spectroscopy, X-ray Diffraction (XRD), Field emission scanning electron microscopy (FESEM), Fourier Transform Infrared (FTIR) spectroscopy, Transmission Electron Microscopy (TEM), Energy Dispersive X-ray (EDX) and Raman spectroscopy. For optical characteristics, optical absorption, band gap, refractive index, Urbach energy, optical polarizability, oxide ion polarizability, optical basicity, and emission cross-section will be obtained according to the equations.

## 1.7 Thesis Outline

The present thesis is structured into five distinct chapters. The initial chapter serves as an introductory section covering various components such as the study's background, a comprehensive overview of glass, the research's motivating factors, a problem description, the objectives, the scope, and the limitations. The second chapter provides a literature review that provides a critical analysis of the research, providing an overview of the glass and previous studies regarding the structure and optical properties of rare-earth-doped tellurite glass systems.

The third chapter focuses on the melt-quenched method of fabricating neodymium NPs-doped tellurite glass. In the meanwhile, graphene oxide was synthesised via electrochemical exfoliation. Graphene oxide was then reduced using



the reduction technique to produce reduced graphene oxide. In this section, the spray-coating technique is discussed. These materials were examined in order to determine their structural and phase compositions. After glass formation, X-ray diffraction (XRD) analysis and Fourier transform infrared spectroscopy (FTIR) were conducted to verify the amorphous character of the glass and the bonding of the glass structure. Using FESEM and micro-Raman spectroscopy, the morphology and microstructural properties of graphene oxide and reduced graphene oxide on the glass surface were determined. TEM analysis confirmed that the glass samples contained neodymium NPS. Using EDX testing, the atomic composition of GO and RGO was determined. Utilising UV–visible–NIR spectroscopy, the optical properties were determined.

The results and discussion of the structural characterization and optical characteristics of the two glass series are presented in Chapter Four. These glass series are graphene oxide-coated neodymium nanoparticle-doped tellurite glass and reduced graphene oxide-coated neodymium nanoparticle-doped tellurite glass. The fifth chapter concludes this study and makes suggestions for future research.

